INTEROCEPTIVE INFORMATION OF PHYSICAL VIGOR:

OREXIN NEURONS GAUGE CIRCULATING IGF-I

FOR MOTIVATIONAL MOTOR OUTPUT

Jonathan A. Zegarra-Valdivia[1,2,3,4,5], Jansen Fernandes[6], Julio Esparza[1],
Kentaro Suda[1,7], Maria Estrella Fernandez de Sevilla[1,2,5],
Sonia Díaz-Pacheco[1], and Ignacio Torres Aleman[1,2,4]

[1]Cajal Institute (CSIC), Madrid, Spain. [2]CIBERNED, Spain. [3]Universidad Nacional de San Agustín de Arequipa, Perú. [4]Achucarro Basque Center for Neuroscience, Leioa, Spain. [5]PhD Program in Neuroscience, Autonoma University, Madrid, Spain.
[6]Universidade Federal São Paulo, São Paulo, Brazil,
[7]Kobe University Graduate School of Medicine, Kobe, Japan,

Abstract

Brain regulation of bodily functions requires interoceptive feedback signals carrying information about the periphery. As mice with low serum IGF-I levels (LID mice) show reduced spontaneous physical activity, we speculated that body vigor information might be conveyed by circulating IGF-I, a regulator of skeletal muscle and bone mass that enters the brain during physical activity. Since hypothalamic orexin neurons, that are involved in regulating physical activity, express IGF-I receptors (IGF-IR), we hypothesized that these neurons might gauge circulating IGF-I levels. Inactivation of IGF-IR in mouse orexin neurons (Firoc mice) reduced spontaneous activity. Firoc mice maintain normal physical fitness but show anxiety- and depressive-like behaviors that seems to interfere with the rewarding effects of exercise, as they were less sensitive to the rewarding actions of exercise. Further, in response to exercise, Firoc mice showed reduced activation of hypothalamic orexin neurons and ventro-tegmental area (VTA) monoaminergic neurons, as indicated by c-fos staining. Collectively, these results suggest that circulating IGF-I is gauged by orexin neurons to modulate physical activity in part by stimulation of the VTA to motivate motor output. Hence, serum IGF-I may constitute a feedback signal, informing orexin neurons to adapt physical activity to physical vigor.

Introduction

Internal bodily states are transmitted to the brain through interoceptive pathways comprising humoral factors and the peripheral nervous system (Craig, 2002). Many body-to-brain signals have been extensively analyzed concerning their brain targets, actions, and circuits involved (Critchley et al., 2004). These include hunger/satiety, adiposity, posture/muscle tone, or visceral function. Interoceptive signals conveying vigor to brain centers are considered the sum of visceral, musculoskeletal, and sensory inputs, but they may also include humoral factors such as insulin-like growth factor I (IGF-I). Indeed, IGF-I sustains apparent vigor (Ayres, 2020). Circulating IGF-I, mainly derived from the liver (Yakar et al., 1999), is taken up by the brain in response to exercise (Carro et al., 2000) and displays a broad range of effects potentially related to vigor awareness, such as modulation of mood (Santi et al., 2018). Moreover, IGF-I is secreted into the circulation in response to muscle activity (DeVol et al., 1990; Berg et al., 2007), is vital in maintaining muscle (Clemmons, 2009) and bone mass (Yakar et al., 2002), and reflects muscle strength (Bucci et al., 2013). Thus, circulating IGF-I is a potential candidate to inform of muscle/bone status to brain centers in charge of controlling physical activity.

Accordingly, we hypothesize that hypothalamic orexin neurons sense increased entrance of serum IGF-I as a result of increased physical activity (Carro et al., 2000). Significantly, orexin neurons express IGF-I receptors, and their activity is regulated by this growth factor (Zegarra-Valdivia et al., 2020). These neurons are involved in multiple basic homeostatic mechanisms, coupling for instance waking with muscle tone (Burgess and Peever, 2013) and controlling general physical activity (Kiwaki et al., 2004; Kotz, 2006). Further, orexin neurons are involved in motivational behaviors (Mahler et al., 2014), and physical activity acts as a rewarding stimulus (Greenwood et al., 2011).

Based on the above considerations, we hypothesize that IGF-I input to orexin neurons conveys physical vigor information. In turn, orexin neurons would sustain physical activity by modulating muscle tone and conveying vigor status to reward areas to positively modulate physical activity. In this way, physical fitness would be linked to well-being. We now report that IGF-I is gauged by orexin neurons, which in turn couple motivation with physical activity by signaling onto the ventral tegmental area (VTA), which is involved in the rewarding aspects of physical exercise (Medrano et al., 2021).

Results

Serum IGF-I modulates physical activity through orexin neurons.

Mice with low serum IGF-I levels (LID mice, Figure 1A) display a disparity of brain deficits and abnormal behaviors (Trejo et al., 2007; Zegarra-Valdivia et al., 2019). We assessed spontaneous activity of LID female mice by housing them in cages with free access to a running wheel and found that they showed reduced spontaneous activity as compared to control littermates (Figure 1B). We use only females in these experiments because they display significantly higher spontaneous activity than males (Suppl Fig. 1A, B). Since treatment with IGF-I for over a month restored physical activity levels in female LID mice (Figure 1C), it seems that systemic IGF-I is involved in regulation of spontaneous activity.

Next, we analyzed orexin neurons as possible targets of circulating IGF-I since these neurons are involved in regulation of physical activity (Kosse et al., 2017). We observed that mice lacking IGF-I receptors in orexin neurons (Firoc mice) also showed diminished spontaneous activity (Figure 1D). The decrease is concentrated in the active phase (Figure 1E), as also seen in LID mice (Suppl Fig. 1C). Reduced spontaneous activity in Firoc mice was consistent along time, as they showed this deficit for at least 6 months (Figure 1F). Since activation of orexin neurons is required for spontaneous physical activity (Kosse et al., 2017), we next inhibited them using DREADDi-expressing viruses in Orexin-Cre mice. Administration of CNO to these mice resulted in reduced spontaneous physical activity (Figure 1G), confirming a direct link between activity of orexin neurons and spontaneous physical activity.

Conversely, as orexin neurons are activated by exercise (Martins et al., 2004), we tested whether exercise activates these neurons in Firoc and LID mice using c-fos immunostaining as a surrogate of neuronal activation (Figure 2A). Firoc mice with free access to the running wheel for 1 hour, showed a significantly lower number of double-labeled orexin^{+}/c-fos^{+} cells in the lateral hypothalamus (LH) 2 hours after exercising (Figure 2B). That circulating IGF-I is essential for activation of orexin neurons by exercise was confirmed in LID mice submitted to the same running protocol. Indeed, LID mice also showed reduced orexin^{+}/c-fos^{+} cells in the LH (Figure 2C). The number of orexin neurons was not significantly different in Firoc and LID mice as compared to their respective controls (Suppl Fig 1D,E).

IGF-I modulates the rewarding aspects of physical activity.

Since Firoc mice show unaltered body weight (Suppl Fig 2A) and muscle mass, normal strength (Suppl Fig 2B-E), intact motor coordination (Suppl Fig 2F), and similar physical activity than controls (Suppl Fig 2G), we analyzed their mood status to determine whether they present motivational disturbances that could explain their lower level of physical activity. Behavioral analysis of Firoc mice (Suppl Fig 3) evidenced a depressive-like and anxiety-like behavior, as determined by the forced swim test and elevated plus maze, respectively (Figure 3A, B). Interestingly, anxiety levels were normal in younger Firoc mice (not shown), suggesting that mood disturbances develop gradually. In addition, Firoc mice presented normal social affiliation but a reduced social novelty/preference (Figure 3C, D). The latter indicates reduced motivation and suggests reduced rewarding effects of social interactions. A relatively similar behavioral pattern was observed in LID mice regarding anxiety but not depressive-like behavior (Figure 3E, F). LID mice also present normal social affiliation and reduced social novelty/preference (Figure 3G, H).

Since the VTA forms part of the reward circuitry (Morales and Margolis, 2017) and is involved in the rewarding aspects of exercise (Medrano et al., 2021), we determined whether IGF-I modulates the activity of VTA neurons. After systemic administration of IGF-I (1 μg/g, ip) to wild-type mice, we determined 2 hours later the number of TH^+ cells expressing c-fos in the VTA (Herrera et al., 2016). IGF-I significantly increased the number of double-labeled TH^+/c-fos^+ cells compared to saline-injected mice (Figure 4A, B). We then analyzed whether Firoc and LID mice show disturbed activation of monoaminergic VTA neurons in response to exercise (1 hour running in the wheel, 2 hours before sacrifice). Firoc mice display significantly reduced c-fos^+ immunostaining in TH^+ cells (Figure 4C, D). Conversely, LID mice showed more double labelled c-fos^+/TH^+ cells compared to controls (Figure 4E). Number of TH^+ cells did not differ between groups (Suppl Fig 4). Nonetheless, the rewarding effects of exercise were attenuated in both Firoc and LID mice, as determined by the conditioned running place preference test. Indeed, both Firoc and LID mice spent significantly less time in the running chamber than control littermates (Figure 5G,H).

Based on the above observations, we treated LID and Firoc mice with SKF82958, a dopamine receptor 1 (DA1) agonist (0.1mg/kg, ip) to ameliorate their possibly reduced dopaminergic tone. However, the dopamine agonist recovered spontaneous physical

activity only in LID mice (Figure 5A, B), showing no effects in Firoc mice (Figure 5C, D).

Discussion

It has been shown that the liver produces hormones that regulate food intake by acting not only on the hypothalamus but also on reward circuitries (Soberg et al., 2017). The present results indicate that circulating IGF-I, produced mainly by the liver (Yakar et al., 1999), influences physical activity acting in part through hypothalamic orexin neurons and the VTA, a component of the reward system. Thus, serum IGF-I deficient mice show less spontaneous activity that is ameliorated by exogenous IGF-I or dopaminergic drugs. Taken together with the observation that IGF-I stimulates VTA neurons (c-fos staining), it seems that the activity of VTA neurons involved in the rewarding aspects of physical activity is modulated by IGF-I.

Additional observations in mice with blunted IGF-IR activity in orexin neurons (Firoc mice) indicate that part of IGF-I actions for motivating physical activity are exerted by modulating orexin activity and their output to monoaminergic neurons at the VTA. Of note, a dopaminergic agonist in Firoc mice did not normalize their spontaneous physical activity. Based on these data, we speculate that circulating IGF-I acts on different subpopulations of VTA neurons (Lammel et al., 2014; Beier et al., 2019) through direct and indirect pathways. The indirect pathway includes IGF-I input through orexin neurons that in turn modulate the VTA. In the absence of this input, this VTA subpopulation is negatively affected by physical activity (Figure 6), as Firoc mice show decreased VTA activation after exercise. A second subpopulation may be directly activated by IGF-I (IGF-I activates c-fos in the VTA), but not by orexin. We speculate that in turn, this second subpopulation modulates physical activity through the IGF-I/orexin-dependent VTA population as the dopamine agonist acts only in LID, but not in Firoc mice (Figure 6). Local connections between different VTA subpopulations have been shown of functional impact in reward (Morales and Margolis, 2017). In agreement with these observations, we previously documented that physical activity stimulates the entrance of serum IGF-I into the brain (Carro et al., 2000), and that circulating IGF-I directly modulates hypothalamic orexin neurons (Zegarra-Valdivia et al., 2020).

Based on these observations, we speculate that physical vigor, as reflected by muscle/bone mass, may be centrally gauged by conveying information through serum

IGF-I to brain regions involved in controlling physical activity (orexin neurons) and its emotional processing (VTA neurons). As discussed elsewhere, the rewarding effects of exercise are probably related to the key function of physical fitness in survival (Erikssen, 2001).

Proper integration of body and mind is paramount for well-being, with inner bodily sensations impinging on emotions in a continued crosstalk (Craig, 2002). An important arm of this body-to-brain signaling is provided by hormones that modulate brain function in multiple ways. The best-studied peripheral-to-brain loop is probably the one involved in energy homeostasis/fat mass, where hormones such as insulin, and many others, exert fine regulatory actions in multiple brain nuclei involved in the central regulation of energy partitioning (Kim et al., 2018). Muscle tissue, which makes the bulk of the body, should also inform brain centers to maintain physical activity according to its resources. However, little is known of the hormonal influence of muscles on brain centers, although diverse myokines have been described to act in the central nervous system (Wrann et al., 2013). We consider that our observations suggest the existence of an IGF-I/orexin loop whereby physical activity adapts to muscle mass in a virtuous cycle. Specifically, physical activity increases IGF-I input to orexin neurons, which in turn assures muscle tone, motivation to move, and even proper energy allocation, as these neurons are essential integrators of peripheral glucose metabolism (Yamanaka et al., 2003).

A recent incorporation to the body-brain dialog is the gut microbiome, that modulates higher brain function in different ways (Mayer et al., 2015). Interestingly, the microbiome increases serum IGF-I levels probably through the production of short chain fatty acids (Yan et al., 2016). Thus, we speculate that the microbiome also participates in modulating the information about physical vigor to the brain acting through neuroendocrine mediators (Cussotto et al., 2018), such as IGF-I. Based on the present observations, we speculate that microbe-originated metabolites such as short-chain fatty acids upregulating serum IGF-I will induce positive mood as recently found for depressive mood regulation by the microbiome (Chevalier et al., 2020) .

These observations may provide an explanation for individual differences in willingness to exercise that could result in faulty long-term adherence to intervention programs of physical activity, a currently advocated therapeutic strategy for multiple conditions (Nunan, 2016). Since exercise behavior may be in part genetically determined (Herring et al., 2014), it could be related to the ability of IGF-I to signal

onto orexin neurons. Thus, individuals with lower IGF-I input to these neurons would show less motivation to exercise. Appropriate serum IGF-I input to orexin neurons will assure a proper level of physical activity, preventing in this way muscle mass loss, as seen in age-associated sarcopenia. We speculate that the latter may be in part due to inappropriate IGF-I input to orexin neurons in old age (Zegarra-Valdivia et al., 2021).

In summary, our results indicate that serum IGF-I enters the brain in response to exercise and is involved in its rewarding effects by modulating VTA neurons through a direct and indirect pathway. The latter involves orexin neurons in the hypothalamus. Further work is needed to more accurately identify VTA circuitries affected by IGF-I and orexin. Indeed, local IGF-I is known to participate in modulation of VTA circuits (Pristera et al., 2019) while orexin projections to VTA have been started to be charted (Baimel et al., 2017).

Materials and Methods

Animals. Adult female Firoc mice (25-32 g, 4-9 months old; Cajal Institute, Spain) and their littermates, LID female mice (liver IGF-1 deficient, congenic with C57BL/6J mice), and wild type C57BL/6J mice of similar ages were housed in standard cages (48 × 26 cm2), 4 - 5 animals per cage. A mixed group (male and female mice) was used where it is specified. Mice were kept in a room with controlled temperature (22°C) under a 12-12h light-dark cycle, fed with a pellet rodent diet, and water ad libitum. All experimental protocols were performed during the light cycle between 13 pm - 17 pm. Animal procedures followed European guidelines (2010/63/EU) and were approved by the local Bioethics Committee (Madrid Government).

Behavioral tests

*Running wheel activity***:** We use a standard polycarbonate cage with a 25 cm diameter running wheel made of stainless steel and low friction connected to a magnetic counter that measures each turn (CIBERTEC, Spain). We use these cages in two sets of experiments, in short-term running (2 weeks), or in long-term running (6 months). The total amount of running is display as total revolutions or running speed, respectively. Running speed was determined for each bout by multiplying the number of revolutions of the wheel in that bout by the wheel circumference and dividing by the bout length.

*Rotarod***:** Animals were familiarized with the device two days before the test. On that day, 4 trials were carried out in which the mouse was placed on the rotating rod, and the speed gradually increased from 4 to 40 rpm for 5 minutes, with 10 minutes between

each test. Time was recorded while mice hold on the rod until they fell or took a full turn. The performance of each mouse was obtained by making the average of the four trials (Al-Mahdawi et al., 2006). Both sexes were included.

*Open Field***:** Animals were introduced in a space of 42 x 42 x 30 cm (AccuScan Instruments) for 10 minutes. Time in the center, as well as the total distance traveled, was quantified automatically by the Versamax program (AccuScan Instruments). Time in the middle of the open field was used as a measure of basal anxiety (Rodgers et al., 1997). Both sexes included.

*Running Reward Conditioned Place Preference***:** The conditioned place preference (CPP) is a standardized tool used to study motivational effects of drugs and non-drugs interventions. In this protocol, we used the running wheel as a reward stimulus in mice as described elsewhere (Fernandes and Fulton, 2016). Briefly, animals were free to run for 3 weeks in horizontal running wheels in their home cages. After that, mice were subjected to a pretest CPP task using a three-chamber maze; a white compartment with black dots, a white compartment with gray vertical lines, and separated each by a neutral center black compartment. Animals spent 5 minutes in each compartment for habituation, and then 15 min of exploring the three chambers. We measure the total time spent in each chamber and use the preference chamber as non-rewarding, and the non-preference as the rewarding chamber. The next day we started 14 days of conditioning program of access to the running wheels or not, interpolated. Mice had 2h access in their home cages to a running wheel (paired trial), or a locked running wheel (unpaired trial), and were then confined to either the black or white compartments of the CPP apparatus for 30 min. On day 15, animals were put in the apparatus for the post-test, again for 15 min of free exploring. The proportion of time spent on the paired side (running chamber) was compared to the total time obtained during the pretest (non-preference chamber).

For double orexin/c-fos or TH/c-fos immunostainings, a sub-group of animals were submitted to free running wheel for one hour for 5 days, as the previous conditioning context. The last day, 2h after running, mice were sacrificed, and their brains processed for immunohistochemistry.

Social behavior: Social behavior include both rewarding and motivational processes (Trezza et al., 2011; McCall and Singer, 2012). We studied social affiliation and social novelty/preference as described by others (Kaidanovich-Beilin et al., 2011).

Inverted screen test: This test consists of a 43 cm square of wire mesh with 12 mm squares of 1mm diameter. The screen is surrounded by a 4 cm deep wooden beading to prevent that the mice climb to the other side of the mesh. We place the mouse in the center of the wire mesh screen and rotate it for 2 min or until it falls down. The test is used to study the muscular strength of the four legs of the animal. Both sexes included.
Weight test: This test includes seven weights (20-95 grams). Mice are hold by the base of the tail and allowed to grasp the different weights. A hold of three seconds is the criterion. If the mouse drops the weight in less than 3 sec, the time is recorded. Both sexes included.
Forced Swim Test: To assess depressive-like behavior, we use the forced swim test (Au - Can et al., 2012). Mice were placed in a glass cylinder (12 cm diameter, 29 cm height) filled with water (23°C) to a height of 15 cm (to avoid climbing). The animals keep swimming until they give up, or they alternated between swimming and floating. A 6 min test session was video recorded and the last 4 min were scored (immobility time; (Munive et al., 2019).
Elevated Plus Maze: To assess anxiety-like behavior, animals were introduced in the center of an elevated plus-maze for 5 min. The maze was 40 cm from the floor with two opposing protected (closed) arms of 30 cm (length)×5 cm (wide)×15.25 (height), and two opposing unprotected (open) arms (30×5×0). Time in the open and closed arms, as well as the number of entries in each arm, was recorded with an automated video-tracking system (Video Tracking Plus Maze Mouse; Med Associates, USA) as already indicated (Zegarra-Valdivia et al., 2019).
Evaluation of muscle mass. Computerized tomography (CT) was used to measure muscle mass using procedures described in detail elsewhere (Pasetto et al., 2018). Briefly, mice were anesthetized by Isofluorane (2.5% flow rate) and kept under at 2.5%. Animals were positioned prone with limbs lateral from the torso for a uniform CT acquisition. Image acquisitions were performed using the Albira II SPECT/CT (Bruker BioSpin PCI) with 600 projections. The X-ray source was set to a current of 400 μA and voltage of 45 kVp. Images were reconstructed using the FBP (Filtered Back Projection) algorithm via the Albira Suite 5.7., reconstructor using "Standard" parameters. These combined acquisition and reconstruction settings produce a final image with 125 μm isotropic voxels. Images were segmented using PMOD v3.3 software according to tissue density-first for total volume. The distance from the upper extremity of the tibia to the medial malleolus (length of the tibia, L), and the perpendicular distance from the

half-length of the tibia to the external margin of the hind limb muscle (thickness of the muscle, T) were measure. T and L measures were acquired by keeping the z axis fixed on the plane where the patella and the upper extremity of tibia were clearly identified. The Index of Muscle Mass (IMM) was defined as the ratio between T and L.

Drug administration. IGF-I was dissolved in saline and intraperitoneally (ip) injected (1µg/g body weight). Mice were processed for immunocytochemistry (see below) two hours after ip IGF-I injection, as described below. SKF82958 (Santa Cruz Biotechnology), a Dopamine Receptor 1 agonist, was administered for 2 weeks at 0.1mg/kg, ip, 30 minutes before the dark phase. Control mice receive saline. Clozapine-N-oxide (CNO) from Tocris at 2mg/kg dissolved in saline 0.9% was injected intraperitoneally 40 min before test sessions.

Immunocytochemistry. Animals were anesthetized with pentobarbital (50 mg/kg) and perfused transcardially with saline 0.9% and then 4% paraformaldehyde in 0.1 M phosphate buffer, pH 7.4 (PB). Coronal 50-µm-thick brain sections were cut in a vibratome and collected in PB 0.1 N. Sections were incubated in permeabilization solution (PB 0.1N, Triton X-100, NHS 10%), followed by 48 hours incubation at 4°C with primary antibody (1:500) in blocking solution (PB 0.1N, Triton X-100, NHS 10%). Antibodies used in this study include rabbit polyclonal c-Fos (Abcam ab190289), orexin polyclonal goat antibody (Santa Cruz 8070), orexin polyclonal rabbit antibody (Abcam ab 6214), and monoclonal tyrosine hydroxylase (TH) mouse antibody (Millipore, MAB318). Followed by goat polyclonal - Alexa Fluor (488 / 594) as secondary antibody (1:1000). Finally, a 1:1000 dilution in PB of Hoechst 33342 was added for 5 minutes. Slices were rinsed several times in PB, mounted with gerbatol mounting medium, and allowed to dry. Omission of primary antibody was used as control.

Cell Image Analysis. Images were taken from the VTA and LH in a confocal microscope (Leica, Germany) using 20X magnification for c-fos. For double-stained TH/c-fos or orexin/c-fos cell counting, four sections per animal were scored using the MATLAB analysis (Dima et al., 2011). First, confocal images were segmented via k-means clustering with the number of clusters set to 5 ($k = 5$) using MATLAB to obtain binary masks for each channel dividing background from the foreground. Red channel masks (TH or Orexin antibody) were further processed by individualizing unconnected regions, putative neurons, and eliminating isolated components with areas smaller than 25 μm^2. The number of neurons in each mask was manually assessed. Green channel

masks (c-fos antibody) were also visually inspected to ensure proper segmentation. Red and green channels were superposed to study the area of co-localization.

For each segmented neuron (red channel), the fraction of its area that co-localized with c-fos antibody (green channel) was measured as an indirect quantification of the amount of c-fos present in that neuron. We referred to this fraction as the co-localization index. The co-localization index of each image was computed as the mean co-localization index of the neurons present in that image. Lastly, the final co-localization index for each condition was computed as the mean co-localization index of all the images belonging to that condition.

Images with only secondary antibody staining were used to check specificity of the secondary antibody (Burry, 2011) and segmented as described above. Specificity was evaluated by measuring the segmented area of the receptor and the number of segmented neurons, comparing the results with tissue images that underwent a complete immunohistochemistry protocol.

Viral constructs. For chemogenetic experiments using DREADD, a viral construct (pAAV-hSyn-DIO-hM4D(Gi)-mCherry ; AAV5; 8.6 x 10^{12} viral infective units/ml) was locally injected bilaterally to inactivate orexin-cre neurons in Orexin-Cre mice. As control virus, we used pAAV-hSyn-DIO-mCherry (AAV5). Both viral constructions were obtained from Addgene. Clozapine N-Oxide (CNO, 2mg/kg dissolved in saline 0.9%) was administered ip and 40 min later behavior was assessed, CNO efficacy in orexin neurons was confirmed in acute slices obtained from injected mice as documented before (Fernandez de Sevilla et al., 2020).

Surgery. For surgeries, mice were anaesthetized with isoflurane (Zoetis) administered with a nose mask (David Kopf Instruments, France), and placed on a stereotaxic frame (Stoelting Co) on a heating pad and tape in their eyes to protect them from light. For viral expression, mice were injected with a 5 µl Hamilton syringe bilaterally into the orexin nuclei (AP= -1.4; ML= ± 0.9; DV= -5.4) 4 weeks before experiments. For DREADDi viral expression, 300 nl were bilaterally infused at a rate of 100 nl/min and the Hamilton syringe withdrawn 10 min later.

Statistics. Statistical analysis was performed using Graph Pad Prism 6 software (San Diego, CA, USA). Depending on the number of independent variables, normally distributed data (Kolmogorov-Smirnov normality test), and the experimental groups compared, we used either Student's t-test or two-way ANOVAs by Sidak's multiple comparison test. For non-normally-distributed data, we used the Mann-Whitney U test

to compare two groups, Kruskall-Wallis or Friedman test, with Dunn's multiple comparisons for multiple groups. The sample size for each experiment was chosen based on previous experience and aimed to detect at least a $p<0.05$ in the different tests applied, considering a reduced use of animals. Results are shown as mean ± standard error (SEM) and p values coded as follows: *$p< 0.05$, **$p< 0.01$, ***$p< 0.001$.

ACKNOWLEDGMENTS

We are thankful to M. García for technical support. J.A. Zegarra-Valdivia acknowledges the financial support of the National Council of Science, Technology and Technological Innovation (CONCYTEC, Perú) through the National Fund for Scientific and Technological Development (FONDECYT, Perú). J. Fernandes received a post-doc fellowship from Fundação de Amparo à Pesquisa do Estado de São Paulo (FAPESP: # 2017/14742-0; # 2019/03368-5). This work was supported by a grant from Ciberned, by a CAM project (Neurodegs), and from SAF2013-40710-R and PID2019-104376RB-I00 (AEI/FEDER, UE).

CONFLICT OF INTEREST

The authors declare no conflict of interests.

AUTHOR CONTRIBUTIONS

J.A. Zegarra-Valdivia designed and conducted experiments, prepared figures, results, and wrote part of the manuscript, J. Fernandez, J. Esparza, K. Suda, and M.E. Fernandez de Sevilla conducted experiments, J. Pignatelli and S. Diaz helped with experiments. I Torres Aleman designed the study and wrote the manuscript.

References

Al-Mahdawi S, Pinto RM, Varshney D, Lawrence L, Lowrie MB, Hughes S, Webster Z, Blake J, Cooper JM, King R, Pook MA (2006) GAA repeat expansion mutation mouse models of Friedreich ataxia exhibit oxidative stress leading to progressive neuronal and cardiac pathology. Genomics 88:580-590.

Au - Can A, Au - Dao DT, Au - Arad M, Au - Terrillion CE, Au - Piantadosi SC, Au - Gould TD (2012) The Mouse Forced Swim Test. JoVE:e3638.

Ayres JS (2020) The Biology of Physiological Health. Cell 181:250-269.

Baimel C, Lau BK, Qiao M, Borgland SL (2017) Projection-Target-Defined Effects of Orexin and Dynorphin on VTA Dopamine Neurons. Cell Reports 18:1346-1355.

Beier KT, Gao XJ, Xie S, DeLoach KE, Malenka RC, Luo L (2019) Topological Organization of Ventral Tegmental Area Connectivity Revealed by Viral-Genetic Dissection of Input-Output Relations. Cell Reports 26:159-167.e156.

Berg U, Gustafsson T, Sundberg CJ, Kaijser L, Carlsson-Skwirut C, Bang P (2007) Interstitial IGF-I in exercising skeletal muscle in women. Eur J Endocrinol 157:427-435.

Bucci L et al. (2013) Circulating levels of adipokines and IGF-1 are associated with skeletal muscle strength of young and old healthy subjects. Biogerontology 14:261-272.

Burgess CR, Peever JH (2013) A noradrenergic mechanism functions to couple motor behavior with arousal state. Curr Biol 23:1719-1725.

Burry RW (2011) Controls for immunocytochemistry: an update. J Histochem Cytochem 59:6-12.

Carro E, Nunez A, Busiguina S, Torres-Aleman I (2000) Circulating insulin-like growth factor I mediates effects of exercise on the brain. J Neurosci 20:2926-2933.

Chevalier G, Siopi E, Guenin-Macé L, Pascal M, Laval T, Rifflet A, Boneca IG, Demangel C, Colsch B, Pruvost A, Chu-Van E, Messager A, Leulier F, Lepousez G, Eberl G, Lledo P-M (2020) Effect of gut microbiota on depressive-like behaviors in mice is mediated by the endocannabinoid system. Nature Communications 11:6363.

Clemmons DR (2009) Role of IGF-I in skeletal muscle mass maintenance. Trends Endocrinol Metab 20:349-356.

Craig AD (2002) How do you feel? Interoception: the sense of the physiological condition of the body. Nat Rev Neurosci 3:655-666.

Critchley HD, Wiens S, Rotshtein P, Ohman A, Dolan RJ (2004) Neural systems supporting interoceptive awareness. Nat Neurosci 7:189-195.

Cussotto S, Sandhu KV, Dinan TG, Cryan JF (2018) The Neuroendocrinology of the Microbiota-Gut-Brain Axis: A Behavioural Perspective. Frontiers in Neuroendocrinology 51:80-101.

DeVol DL, Rotwein P, Sadow JL, Novakofski J, Bechtel PJ (1990) Activation of insulin-like growth factor gene expression during work-induced skeletal muscle growth. American Journal of Physiology-Endocrinology and Metabolism 259:E89-E95.

Dima AA, Elliott JT, Filliben JJ, Halter M, Peskin A, Bernal J, Kociolek M, Brady MC, Tang HC, Plant AL (2011) Comparison of segmentation algorithms for fluorescence microscopy images of cells. Cytometry A 79:545-559.

Erikssen G (2001) Physical fitness and changes in mortality: the survival of the fittest. Sports Med 31:571-576.

Fernandes MFA, Fulton S (2016) Running Reward Conditioned Place Preference Task. Bio-protocol 6:e1816.

Fernandez de Sevilla M, Pignatelli J, Mendez P, Zegarra-Valdivia J, Torres Alemán I (2020) Insulin-Like Growth Factor I Modulates Vulnerability to Stress Through Orexin Neurons. bioRxiv:2020.2002.2010.941377.

Greenwood BN, Foley TE, Le TV, Strong PV, Loughridge AB, Day HE, Fleshner M (2011) Long-term voluntary wheel running is rewarding and produces plasticity in the mesolimbic reward pathway. Behav Brain Res 217:354-362.

Herrera JJ, Fedynska S, Ghasem PR, Wieman T, Clark PJ, Gray N, Loetz E, Campeau S, Fleshner M, Greenwood BN (2016) Neurochemical and behavioural indices of exercise reward are independent of exercise controllability. Eur J Neurosci 43:1190-1202.

Herring MP, Sailors MH, Bray MS (2014) Genetic factors in exercise adoption, adherence and obesity. Obes Rev 15:29-39.

Kaidanovich-Beilin O, Lipina T, Vukobradovic I, Roder J, Woodgett JR (2011) Assessment of social interaction behaviors. J Vis Exp.

Kim K-S, Seeley RJ, Sandoval DA (2018) Signalling from the periphery to the brain that regulates energy homeostasis. Nature Reviews Neuroscience 19:185.

Kiwaki K, Kotz CM, Wang C, Lanningham-Foster L, Levine JA (2004) Orexin A (hypocretin 1) injected into hypothalamic paraventricular nucleus and spontaneous physical activity in rats. Am J Physiol Endocrinol Metab 286:E551-E559.

Kosse C, Schone C, Bracey E, Burdakov D (2017) Orexin-driven GAD65 network of the lateral hypothalamus sets physical activity in mice. Proc Natl Acad Sci U S A 114:4525-4530.

Kotz CM (2006) Integration of feeding and spontaneous physical activity: role for orexin. Physiol Behav 88:294-301.

Lammel S, Lim BK, Malenka RC (2014) Reward and aversion in a heterogeneous midbrain dopamine system. Neuropharmacology 76 Pt B:351-359.

Lammel S, Hetzel A, Hackel O, Jones I, Liss B, Roeper J (2008) Unique properties of mesoprefrontal neurons within a dual mesocorticolimbic dopamine system. Neuron 57:760-773.

Mahler SV, Moorman DE, Smith RJ, James MH, Aston-Jones G (2014) Motivational activation: a unifying hypothesis of orexin/hypocretin function. Nature neuroscience 17:1298-1303.

Martins PJ, D'Almeida V, Pedrazzoli M, Lin L, Mignot E, Tufik S (2004) Increased hypocretin-1 (orexin-a) levels in cerebrospinal fluid of rats after short-term forced activity. Regul Pept 117:155-158.

Mayer EA, Tillisch K, Gupta A (2015) Gut/brain axis and the microbiota. J Clin Invest 125:926-938.

McCall C, Singer T (2012) The animal and human neuroendocrinology of social cognition, motivation and behavior. Nat Neurosci 15:681-688.

Medrano MC, Hurel I, Mesguich E, Redon B, Stevens C, Georges F, Melis M, Marsicano G, Chaouloff F (2021) Exercise craving potentiates excitatory inputs to ventral tegmental area dopaminergic neurons. Addict Biol 26:e12967.

Morales M, Margolis EB (2017) Ventral tegmental area: cellular heterogeneity, connectivity and behaviour. Nat Rev Neurosci 18:73-85.

Munive V, Zegarra-Valdivia JA, Herrero-Labrador R, Fernandez AM, Aleman IT (2019) Loss of the interaction between estradiol and insulin-like growth factor I

in brain endothelial cells associates to changes in mood homeostasis during peri-menopause in mice. Aging (Albany NY) 11:174-184.

Nunan D (2016) Doctors should be able to prescribe exercise like a drug. BMJ (Clinical research ed) 353:i2468.

Pasetto L, Olivari D, Nardo G, Trolese MC, Bendotti C, Piccirillo R, Bonetto V (2018) Micro-computed tomography for non-invasive evaluation of muscle atrophy in mouse models of disease. PLoS One 13:e0198089.

Pristera A, Blomeley C, Lopes E, Threlfell S, Merlini E, Burdakov D, Cragg S, Guillemot F, Ang SL (2019) Dopamine neuron-derived IGF-1 controls dopamine neuron firing, skill learning, and exploration. Proc Natl Acad Sci U S A 116:3817-3826.

Rodgers RJ, Cao BJ, Dalvi A, Holmes A (1997) Animal models of anxiety: an ethological perspective. Braz J Med Biol Res 30:289-304.

Santi A, Bot M, Aleman A, Penninx BWJH, Aleman IT (2018) Circulating insulin-like growth factor I modulates mood and is a biomarker of vulnerability to stress: from mouse to man. Translational Psychiatry 8:142.

Soberg S, Sandholt CH, Jespersen NZ, Toft U, Madsen AL, von Holstein-Rathlou S, Grevengoed TJ, Christensen KB, Bredie WLP, Potthoff MJ, Solomon TPJ, Scheele C, Linneberg A, Jorgensen T, Pedersen O, Hansen T, Gillum MP, Grarup N (2017) FGF21 Is a Sugar-Induced Hormone Associated with Sweet Intake and Preference in Humans. Cell Metab 25:1045-1053 e1046.

Trejo JL, Piriz J, Llorens-Martin MV, Fernandez AM, Bolos M, LeRoith D, Nunez A, Torres-Aleman I (2007) Central actions of liver-derived insulin-like growth factor I underlying its pro-cognitive effects. Mol Psychiatry 12:1118-1128.

Trezza V, Campolongo P, Vanderschuren LJ (2011) Evaluating the rewarding nature of social interactions in laboratory animals. Dev Cogn Neurosci 1:444-458.

Wrann C-á, White J-á, Salogiannnis J, Laznik-Bogoslavski D, Wu J, Ma D, Lin J-á, Greenberg M-á, Spiegelman B-á (2013) Exercise Induces Hippocampal BDNF through a PGC-1+'/FNDC5 Pathway. Cell Metabolism 18:649-659.

Yakar S, Liu JL, Stannard B, Butler A, Accili D, Sauer B, LeRoith D (1999) Normal growth and development in the absence of hepatic insulin-like growth factor I. Proc Natl Acad Sci U S A 96:7324-7329.

Yakar S, Rosen CJ, Beamer WG, Ackert-Bicknell CL, Wu Y, Liu JL, Ooi GT, Setser J, Frystyk J, Boisclair YR, LeRoith D (2002) Circulating levels of IGF-1 directly regulate bone growth and density. J Clin Invest 110:771-781.

Yamanaka A, Beuckmann CT, Willie JT, Hara J, Tsujino N, Mieda M, Tominaga M, Yagami K, Sugiyama F, Goto K, Yanagisawa M, Sakurai T (2003) Hypothalamic orexin neurons regulate arousal according to energy balance in mice. Neuron 38:701-713.

Yan J, Herzog JW, Tsang K, Brennan CA, Bower MA, Garrett WS, Sartor BR, Aliprantis AO, Charles JF (2016) Gut microbiota induce IGF-1 and promote bone formation and growth. Proc Natl Acad Sci U S A 113:E7554-e7563.

Zegarra-Valdivia JA, Santi A, Fernandez de Sevilla ME, Nunez A, Torres Aleman I (2019) Serum Insulin-Like Growth Factor I Deficiency Associates to Alzheimer's Disease Co-Morbidities. J Alzheimers Dis 69:979-987.

Zegarra-Valdivia JA, Pignatelli J, Fernandez de Sevilla ME, Fernandez AM, Munive V, Martinez-Rachadell L, Nunez A, Torres Aleman I (2020) Insulin-like growth factor I modulates sleep through hypothalamic orexin neurons. FASEB J 34:15975-15990.

Zegarra-Valdivia JA, Fernandes J, Trueba-Saiz A, de Sevilla MEF, Pignatelli J, Suda K, Martinez-Rachadell L, Fernandez AM, Esparza J, Vega M, Nuñez A, Aleman IT (2021) INSULIN-LIKE GROWTH FACTOR I SENSITIZATION REJUVENATES SLEEP PATTERNS IN OLD MICE. bioRxiv:2021.2002.2023.432494.

LEGENDS TO FIGURES

Figure 1: Serum IGF-I regulates physical activity through orexin neurons. A, LID mice have reduced serum IGF-I levels compared to controls (wild type; WT=6, LID=12; ***p<0.0001, Unpaired t-test, sex balanced) **B,** Female LID mice show reduced spontaneous activity when housed with free access to a running wheel (WT=5, LID=10; ***p<0.0001, Two-Way ANOVA). **C,** Differences in running behavior between WT and LID disappear after one-month treatment with IGF-I (WT=4, LID=4; p=0.1131, Two-Way RM ANOVA). **D,** Female mice lacking functional IGF-IR in orexin neurons (Firoc mice) show reduced spontaneous activity compared to control littermates (WT=10, Firoc=9; ***p<0.0001, Two-Way ANOVA). **E,** Firoc mice show reduced activity only during the active phase (WT=8, Firoc=7; **p=0.0024, Two-Way ANOVA). **F,** Firoc mice show reduced activity for at least 6 consecutive months (WT=5, Firoc=5; *p=0.0358, Two-Way RM ANOVA). **G,** Chemogenetic inhibition of orexin neurons with DREADDi virus injected in Orexin-Cre mice (n=50) leads to reduced spontaneous activity as measured in the running wheel. Control mice received a control mCherry virus. Representative diagram of coronal section indicating the LH area where double-injection of DREADDi-expressing viruses was carried out (n=43; **p=0.0018, Two-Way ANOVA).

Figure 2: Running elicits reduced activation of orexin neurons in LID and Firoc mice. A, Both LID and Firoc mice submitted to voluntary wheel running show a reduced number of double-labeled orexin (red)/c-fos (green) cells in the lateral hypothalamus as compared to controls. Bars are 50 µm. **B,** Quantification histograms of double-labeled orexin/c-fos neurons in WT (n=27 fields area of LH, 3 mice) and Firoc (n=13 fields area of LH, 3 mice) show significant differences (*p=0.0167, Unpaired t-test, Welch correction). **C,** Quantification histograms of double-labeled orexin/c-fos neurons in WT (n=16 fields area of LH, 3 mice) and LID (n=25 field area of LH, 3 mice) show significant differences (***p<0.001, Unpaired t-test).

Figure 3: Behavioral disturbances in Firoc and LID mice. A, Depressive-like behavior in Firoc mice, as determined in the forced swim test, was increased (WT=11, Firoc=13; **p<0.001, Unpaired t-test). **B,** Increased anxiety in Firoc mice, as determined in the elevated plus-maze (WT=17, Firoc=15; *p=0.0177, Unpaired t-test). **C,** Social affiliation in Firoc mice was normal, as indicated by the "stranger vs. empty box" test (WT=24, Firoc= 9; ***p<0.001, Two-Way ANOVA). **D**, Social novelty/preference in Firoc mice was disrupted, as indicated by the "new-partner vs. familiar partner" test (WT= 21, Firoc= 9, WT preference **p=0.0085, Firoc preference p=0.9698, Two-Way ANOVA). **E,** As determined in the forced swim test, depressive-like behavior in LID mice was similar in both groups (WT=12, LID=8; p=0.9520, Unpaired t-test). **F,** Increased anxiety is found of LID mice as determined in the elevated plus-maze (WT=13, LID=12; ***p<0.0001, Unpaired t-test, Welch Correction). **F,** Social affiliation in LID mice was normal, as indicated by the "stranger vs. empty box" test (WT=10, LID=11; **p<0.01, Two-Way ANOVA). **G,** Social

intercourse is significantly altered in LID mice, as indicated by the "new-partner vs. familiar" test (WT=14, LID=11; WT preference *p<0.05, LID preference p=0.9531, WT vs. LID new stranger preference, **p=0.0042, Two-Way ANOVA).

Figure 4: IGF-I and exercise modulate the activity of monoaminergic VTA neurons. A, Representative micrographs of double-stained c-fos (green)/TH (red) cells in the VTA of wild-type mice injected with saline or IGF-I (1µg/g body weight, ip; two hours before). Bars are 50 µm. **B,** Quantification histograms of double-labelled c-fos$^{+/}$ TH^{+} cells in VTA (saline n=11 fields, 3 mice; IGF-I mice=15 fields, 3 mice; **p=0.0063, Unpaired t-test). Schematic representation of VTA area (right hand). **C,** Double-stained c-fos$^{+/}$TH^{+} cells in the VTA of Firoc and WT (littermates) after 1 h exercise. Bars are 50 µm. **D,** Quantification histograms of double-labelled c-fos^{+}/TH^{+} cells (WT=19 fields, Firoc=16 fields, 3 mice per group; *p=0.0256, Unpaired t-test). **E,** Double-stained c-fos^{+}/TH^{+}cells in the VTA of LID mice after 1 h exercise. Bars are 50 µm. **F,** Quantification histograms of double-labelled c-fos^{+}/ TH+ cells (WT=4 fields, LID=6 fields, 3 mice per group; p=0.1388, Mann-Whitney t-test). **G,** The rewarding effects of exercise are attenuated in Firoc mice, as seen by significantly reduced time spent in the exercise chamber (WT=16, Firoc=10; *p=0.029, Unpaired t-test). **H,** Place preference is also reduced in LID mice (WT=16, LID=17; **p=0.0049, Unpaired t-test).

Figure 5: Treatment with a dopamine receptor 1 agonist restores spontaneous physical activity in LID, but not in Firoc mice. A, Administration of the D1 agonist SKF82958 (0.1mg/kg, ip) to LID mice significantly increased their spontaneous activity even after treatment ceased (LID saline=10, LID D1 agonist=9; ***p<0.001). **B,** Total activity along time of treatment was increased in SKF82958 -treated LID mice (***p<0.001, Mann-Whitney test). **C,** Firoc mice treated with SKF82958 changed the pattern of spontaneous physical activity (n= 9 per group; p=0.4047, interaction factor=0.0030, day 4 *p=0.0327). **D,** Total activity along time of treatment was decreased in SKF82958 -treated Firoc mice (**p=0.0018).

Figure 6: Schematic representation of the relationships between circulating IGF-I, orexin, and VTA neurons to promote physical activity. After physical activity is increased in response to internal or external stimuli, entrance of circulating IGF-I into the brain is enhanced (Carro et al., 2000). Orexin neurons are activated by IGF-I (Zegarra-Valdivia et al., 2020), and in turn, a subpopulation of monoaminergic (TH^{+}) neurons in the VTA are stimulated to sustain motor output. This population becomes depressed in response to exercise when IGF-I/orexin input is missing (Firoc mice). A second IGF-I/orexin-independent subpopulation, -within at least five subpopulations of dopaminergic VTA neurons (Lammel et al., 2008), that may be responsive to IGF-I, is involved in motivational motor output acting onto the first subpopulation through a dopaminergic-sensitive (DR1 agonist- sensitive) pathway.

Supplementary Figure 1. A, Spontaneous physical activity in male WT mice is lower than in females (males=9, females=15; ***p<0.0001, Two-Way ANOVA). **B,** Total

running differences between males and females (males=9, females=15; ***p<0.0001, Mann-Whitney U test). **C,** LID mice selectively reduced running behavior in the active phase (n=5 per group; ***p<0.0001, Two-Way ANOVA). **D,** Number of orexin$^+$ neurons in LH did not differ between experimental groups (WT=2189 ± 511.6, Firoc=1668 ±482.2; p=0.4359, Mann-Whitney test), and (WT=553.2 ± 90.91, LID=641.3 ± 135.1 cells, p=0.4710, One-Way ANOVA).

Supplementary Figure 2. A, No differences in body weight were seen between Firoc mice and littermates (3-4 months old, WT=18, Firoc=12, p=0.2974, Unpaired t-test). **B,** Firoc mice and littermates have similar muscle mass, as determined by computerized tomography (CT) imaging. A representative CT scan showing the calculation of the length and diameter of the leg muscle. **C,** Quantification histograms of muscle mass index (n=5 per group; p=0.8357, Unpaired t-test). **D,** Performance in the inverted screen test, designed to measure strength in the muscles of the four legs, was similar in Firoc mice and littermates (WT=12, Firoc=18; p>0.999, Mann-Whitney Test). **E,** An additional measure of muscle strength, the weight-lifting test, also indicates similar strength in both experimental groups (WT=12, Firoc=18; p=0.8743, Unpaired t-test). **F,** Motor coordination in the rotarod test was unperturbed in Firoc mice (WT=11, Firoc=16; p=0.6359, Mann-Whitney Test). **G,** Deambulation in the open field test was similar in Firoc and littermates (n=10 per group; p=0.8357, Mann-Whitney Test). We use female and male mice in these behaviors, no differences were found between sexes.

Supplementary Figure 3. Timeline of behavioral experiments. Behavioral analyses started with a social interaction test (affiliation and novelty/preference). Next, a new set of animals were submitted to running for 3 weeks. After that, a pre-CPP test measure was performed. Then, animals were conditioned to the running wheel for 14 days. On day 15 the post-CPP was performed. Four days later, the EPM was carried out, and 4 days later the FST was run with the same group of animals.

Supplementary Figure 4. A, Number of TH$^+$ cells in VTA did not differ between saline (n=1170 ± 245.8) and IGF-I-injected mice (n=775.7 ± 193.4), p=0.2472, Unpaired t-test. **B,** Number of TH$^+$ cells in VTA did not differ between Firoc and wild type (WT) littermates (WT=2189 ± 511.6, Firoc=1668 ±482.2; p=0.4359, Mann-Whitney test). **C,** Number of TH$^+$ cells in VTA are similar between LID and littermates (WT=1193 ± 94.93, LID=1257 ± 104.3; p=0.6571, Mann-Whitney test).

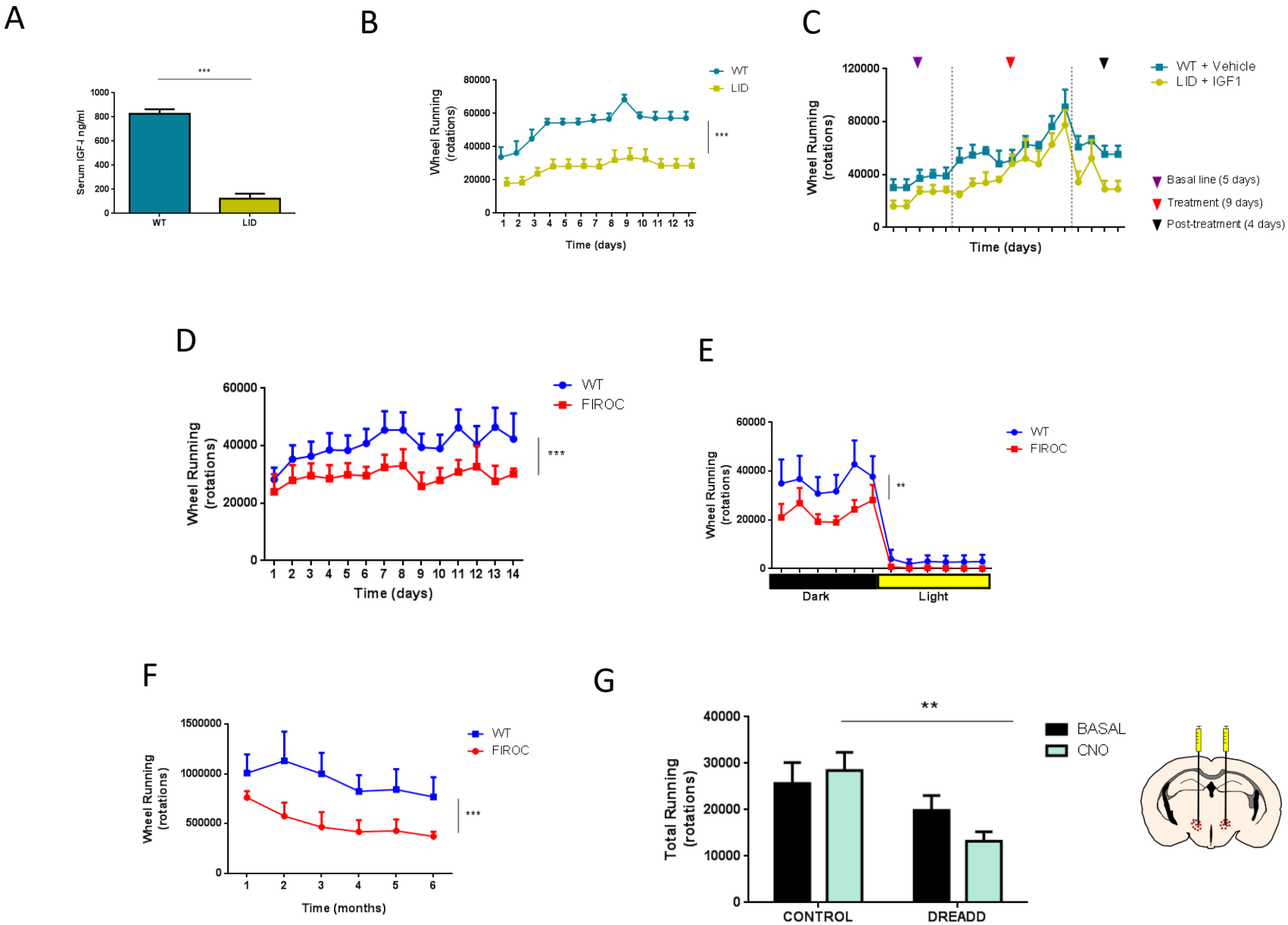
A
Serum IGF-I ng/ml
1000
800
600
400
200
0
***
WT
LID
B
Wheel Running (rotations)
80000
60000
40000
20000
0
1 2 3 4 5 6 7 8 9 10 11 12 13
Time (days)
WT
LID
***
C
Wheel Running (rotations)
120000
80000
40000
0
Time (days)
WT + Vehicle
LID + IGF1
Basal line (5 days)
Treatment (9 days)
Post-treatment (4 days)
D
Wheel Running (rotations)
60000
40000
20000
0
1 2 3 4 5 6 7 8 9 10 11 12 13 14
Time (days)
WT
FIROC
***
E
Wheel Running (rotations)
60000
40000
20000
0
**
Dark
Light
WT
FIROC
F
Wheel Running (rotations)
1500000
1000000
500000
0
1 2 3 4 5 6
Time (months)
WT
FIROC
***
G
Total Running (rotations)
40000
30000
20000
10000
0
**
CONTROL
DREADD
BASAL
CNO

Figure 1

A

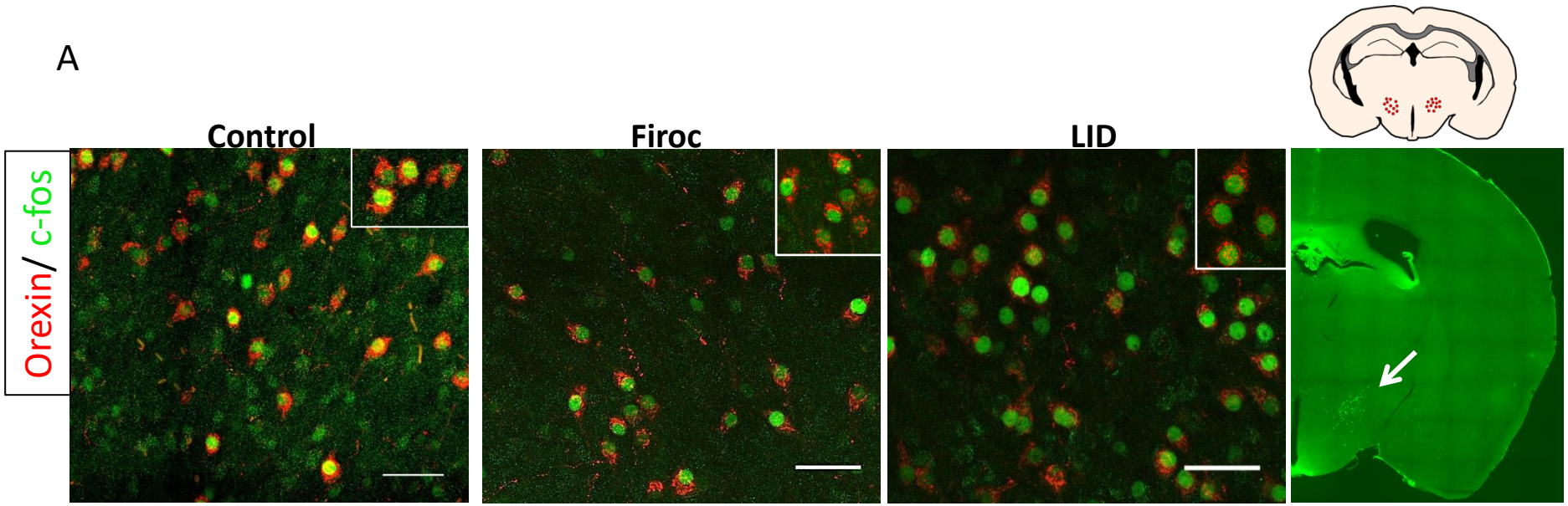
Control
Firoc
LID
Orexin/ c-fos

B

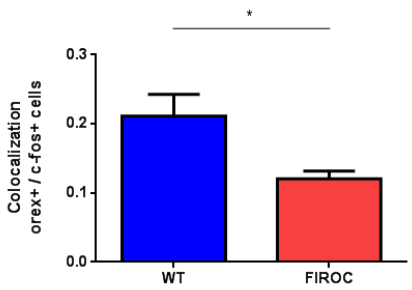
*
Colocalization
orex+ / c-fos+ cells
0.3
0.2
0.1
0.0
WT
FIROC

C

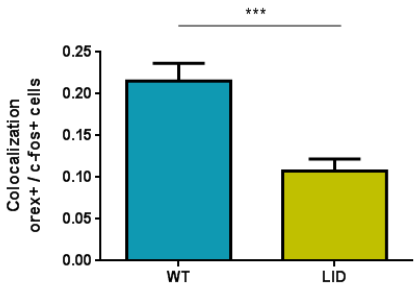
***
Colocalization
orex+ / c-fos+ cells
0.25
0.20
0.15
0.10
0.05
0.00
WT
LID

Figure 2

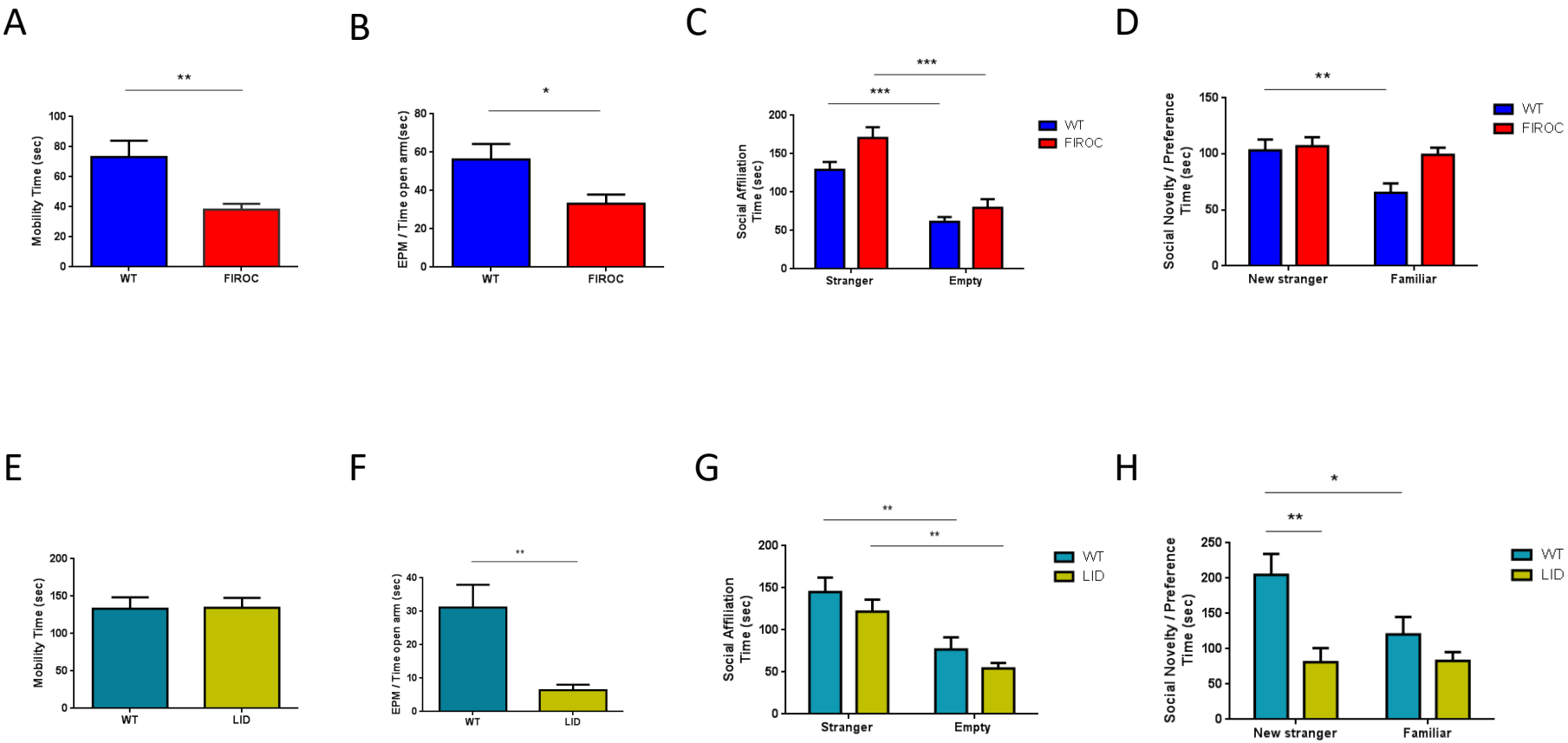
A
Mobility Time (sec)
WT
FIROC
B
EPM / Time open arm(sec)
WT
FIROC
C
Social Affiliation Time (sec)
Stranger
Empty
WT
FIROC
D
Social Novelty / Preference Time (sec)
New stranger
Familiar
WT
FIROC
E
Mobility Time (sec)
WT
LID
F
EPM / Time open arm (sec)
WT
LID
G
Social Affiliation Time (sec)
Stranger
Empty
WT
LID
H
Social Novelty / Preference Time (sec)
New stranger
Familiar
WT
LID

Figure 3

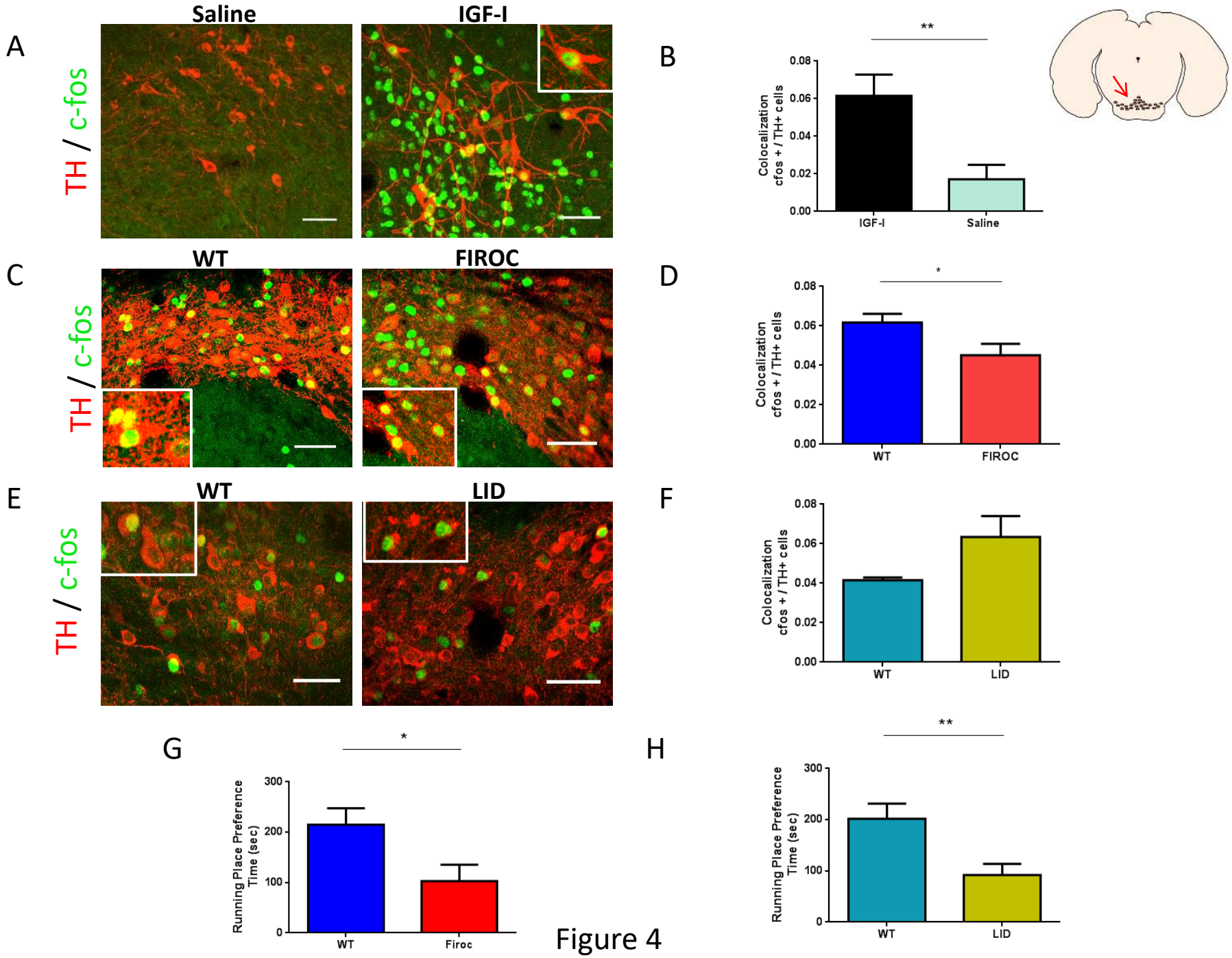
A
Saline
IGF-I
TH / c-fos
B
**
Colocalization cfos + / TH+ cells
0.08
0.06
0.04
0.02
0.00
IGF-I
Saline
C
WT
FIROC
TH / c-fos
D
*
Colocalization cfos + / TH+ cells
0.08
0.06
0.04
0.02
0.00
WT
FIROC
E
WT
LID
TH / c-fos
F
Colocalization cfos + / TH+ cells
0.08
0.06
0.04
0.02
0.00
WT
LID
G
*
Running Place Preference Time (sec)
300
200
100
0
WT
Firoc
H
**
Running Place Preference Time (sec)
300
200
100
0
WT
LID

Figure 4

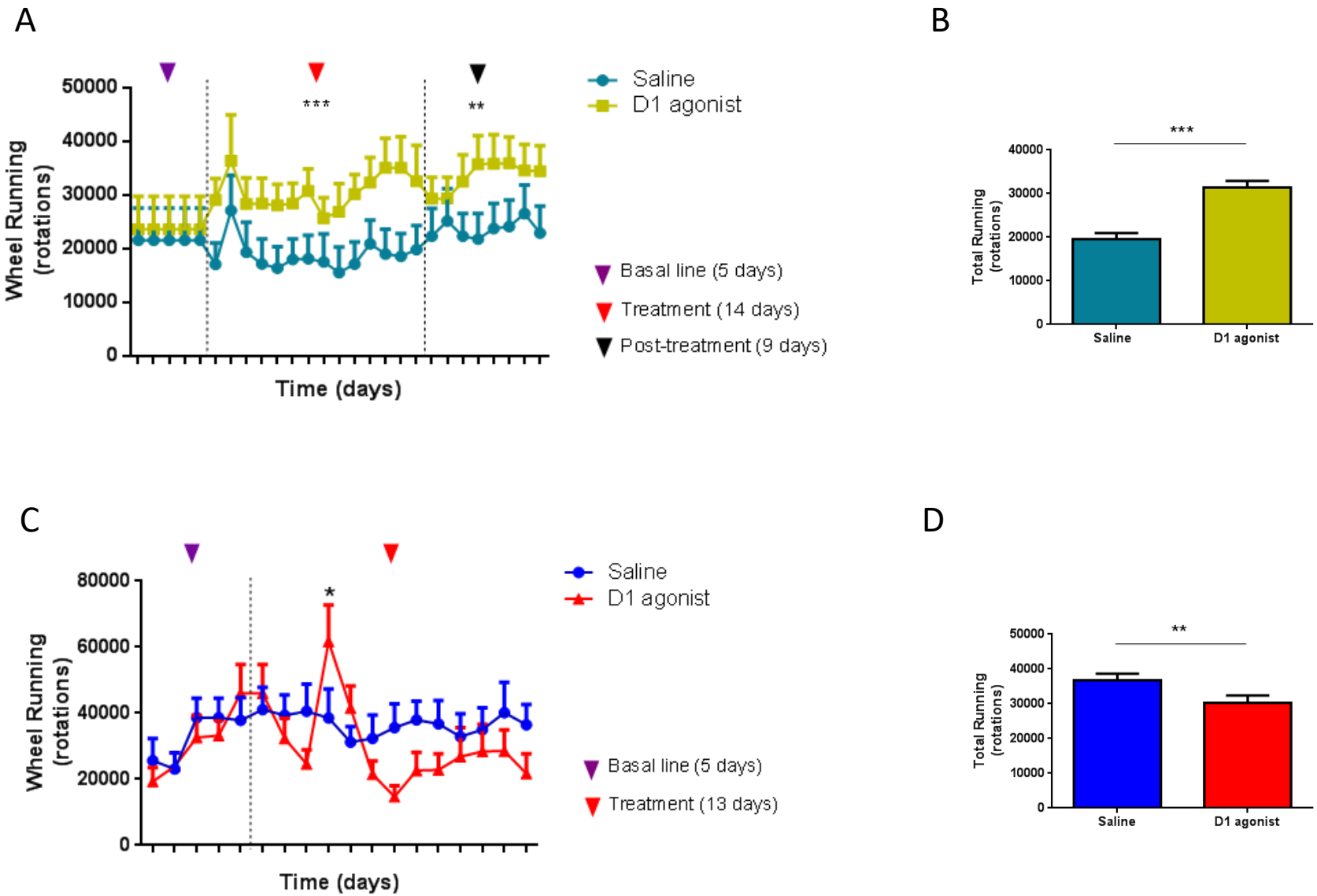
A
Wheel Running (rotations)
50000
40000
30000
20000
10000
0
***
**
Time (days)
Saline
D1 agonist
Basal line (5 days)
Treatment (14 days)
Post-treatment (9 days)
B
Total Running (rotations)
40000
30000
20000
10000
0
***
Saline
D1 agonist
C
Wheel Running (rotations)
80000
60000
40000
20000
0
*
Time (days)
Saline
D1 agonist
Basal line (5 days)
Treatment (13 days)
D
Total Running (rotations)
50000
40000
30000
20000
10000
0
**
Saline
D1 agonist

Figure 5

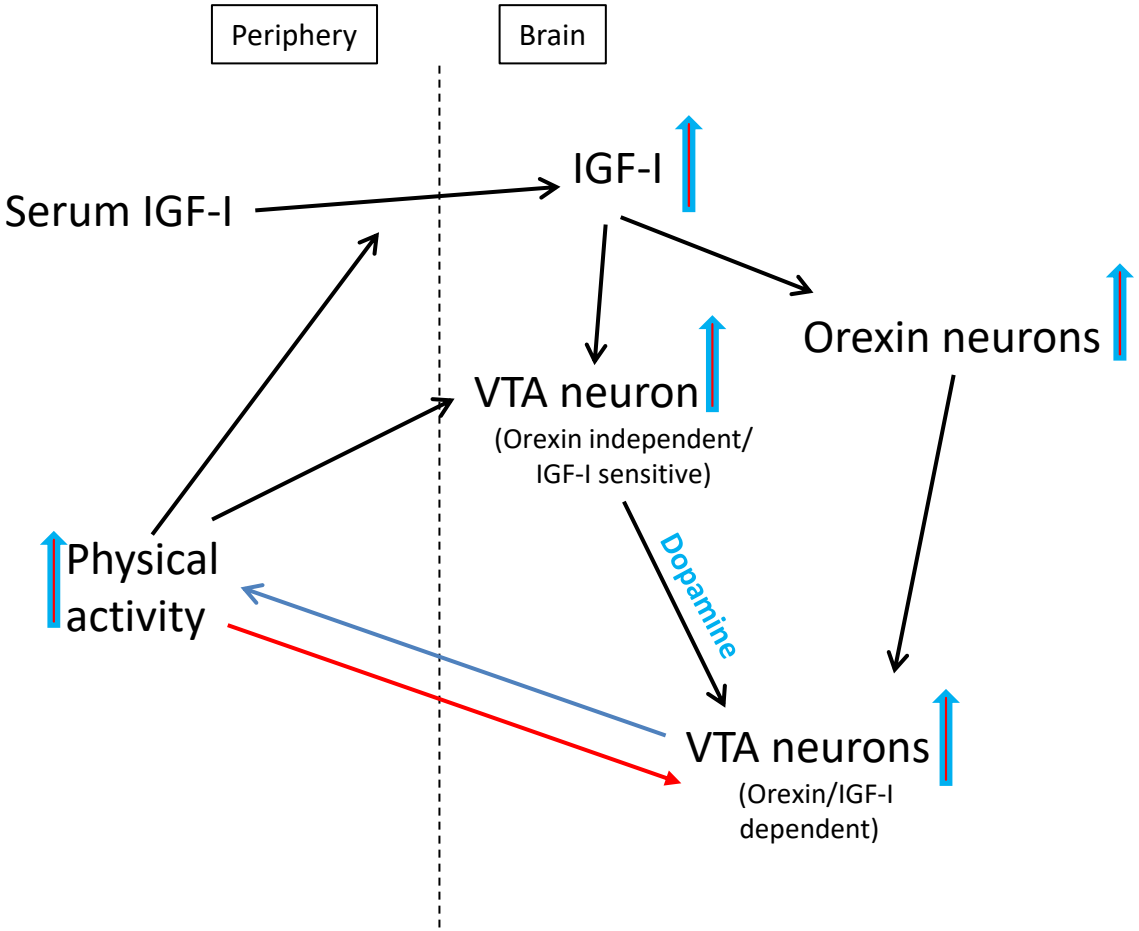
Periphery
Brain
Serum IGF-I
IGF-I
Orexin neurons
VTA neuron
(Orexin independent/
IGF-I sensitive)
Physical
activity
Dopamine
VTA neurons
(Orexin/IGF-I
dependent)

Figure 6